How to observe ^{8}B solar neutrinos in liquid scintillator detectors

A. Ianni [a] D. Montanino [b] F.L. Villante [c]

[a] *Laboratori Nazionali del Gran Sasso and INFN, I-67010 Assergi, Italy*

[b] *Dipartimento di Scienza dei Materiali, Università di Lecce and INFN, I-73100 Lecce, Italy*

[c] *Dipartimento di Fisica, Università di Ferrara and INFN, I-44100 Ferrara, Italy*

Abstract

We show that liquid organic scintillator detectors (e. g., KamLAND and Borexino) can measure the ^{8}B solar neutrino flux by means of the ν_e charged current interaction with the ^{13}C nuclei naturally contained in the scintillators. The neutrino events can be identified by exploiting the time and space coincidence with the subsequent decay of the produced ^{13}N nuclei. We perform a detailed analysis of the background in KamLAND, Borexino and in a possible liquid scintillator detector at SNOLab, showing that the ^{8}B solar neutrino signal can be extracted with a reasonable uncertainty in a few years of data taking. KamLAND should be able to extract about 18 solar neutrino events from the already collected data. Prospects for gigantic scintillator detectors (such as LENA) are also studied.

Key words: Solar neutrinos, neutrino detectors, neutrino mass and mixing
PACS: : 14.60.Lm, 14.60.Pq, 26.65.+t

1 Introduction

Observations of solar neutrinos [1,2,3,4,5,6,7] have offered the first experimental evidence in favor of non-standard effects, in particular neutrino flavor transitions induced by non-zero neutrino masses and mixings. Solar neutrinos have been detected by radiochemical experiments (i. e., Homestake [1], Gallex/GNO [2,3] and SAGE [4]) which give an energy-integrated information on the solar neutrino fluxes, and by real time water Cherenkov detectors (i. e., Kamiokande, Super-Kamiokande [5,6] and SNO [7]) which allow to observe the spectral distribution of solar neutrino events. However, the detection threshold in Cherenkov detectors is limited to about 5 MeV by the radiopurity

of the target mass and, as a consequence, only high energy ^{8}B solar neutrinos spectrum has been measured.

In the next future, liquid organic scintillator detectors, such as KamLAND [8] and Borexino [9,10], will be operating with the goal of measuring the low energy solar neutrino fluxes, in particular ^{7}Be, CNO and *pep* solar neutrinos. The KamLAND experiment is a 1 kT detector located in the Kamioka mine (Japan), at a depth of 2700 m.w.e. of rock, operating continuously since January 2002, with the main goal of measuring the flux of the $\bar{\nu}_e$'s coming from all the Japanese nuclear power plants. This experiment has spectacularly confirmed the so-called Large Mixing Angle (LMA) solution to the solar neutrino problem (see, e. g., [11] for a recent reanalysis). Borexino is a 0.3 kT liquid scintillator detector which is being commissioned at Gran Sasso (Italy), under 3800 m.w.e. of rock, whose main goal is the measurement of the ^{7}Be solar neutrino flux. Moreover, it has been recently proposed to realize a ~ 1 kT liquid scintillator detector, denominated SNO+, at the SNO site (SNOLab, Canada) under 6000 m.w.e. of rock, after the completion of the SNO detector physics program [12]. It is also under discussion the possibility to realize a gigantic ($\geq$ 30kT) liquid scintillator detector, the Low Energy Neutrino Astrophysics (LENA) detector [13], in the Pyhäsalmi mine (Finland) at a depth of 1450 m ($\sim$ 4000 m.w.e.), although other sites (e. g., underwater in the site of Pylos in Greece) have also been proposed. The observation of solar neutrinos in these detectors, through $\nu-$e elastic scattering, is not a simple task, since neutrino events cannot be separated from the background, and it can be accomplished only if the detectors contamination will be kept very low [9]. Moreover, only mono-energetic sources such as ^{7}Be or *pep* neutrinos can be detected, taking advantage of the Compton-like shoulder edge produced in the event spectrum.

In this Letter, we show that organic liquid scintillator detectors can also measure the ^{8}B solar neutrino flux by means of the ν_e charged current interaction with the ^{13}C nuclei naturally contained in the scintillators. The possibility to use ^{13}C as a target for ^{8}B neutrinos was pointed out in the past by [14,15,16]. Here, we propose a technique to tag the solar neutrino events. Namely, we propose to identify the signal by looking at the time and space coincidence with the decay of the produced ^{13}N nuclei. We perform a detailed calculation of the solar neutrino signal and of the background in KamLAND, Borexino and SNO+, showing that these detectors will be able to extract the signal with a reasonable uncertainty in a few years of data taking. It should be stressed that the proposed technique does not involve any modification of the experimental setup, since one expects a background-to-signal ratio of the order of 1 or less even assuming the natural isotopic abundance of ^{13}C ($\sim 1\%$) and the contamination levels already reached in the KamLAND detector [17].

The Letter is organized as follows. In the next section we discuss the neutrino interactions with ^{13}C. In Sec. III we calculate the solar neutrino event rates. In

Sec. IV we analyze the space and time coincidence with the decay of the produced ^{13}N nuclei. Background issues are described in Sec. V. Sec. VI presents the expected sensitivity for KamLAND, Borexino and SNO+ and prospects for LENA. In Sec. VII we draw our conclusions.

2 Neutrino interactions on ^{13}C

The ^{13}C is a stable isotope of carbon with a natural isotopic abundance $I = 1.07\%$. A small amount of ^{13}C is, thus, naturally present in organic liquid scintillators and can be used as a target for neutrino detection. The relevant detection process in our discussion is the charged current (CC) transition to ^{13}N ground state:

$$\nu_{\rm e} + {}^{13}{\rm C} \rightarrow {}^{13}{\rm N}({\rm gnd}) + {\rm e}^- \ . \tag{1}$$

The reaction threshold is $Q = 2.22$ MeV and, thus, only ^{8}B solar neutrinos are detectable (with a neglible contribution from *hep* neutrinos). In liquid scintillators one observes the electron produced in the final state with a visible energy which, neglecting the detector energy resolution, is simply equal to the electron kinetic energy $T_{\rm e}$. The cross section of reaction (1) is known with great accuracy, since it can be deduced from the decay time of ^{13}N. One has [15]:

$$\begin{aligned}\sigma(E_\nu) &= \frac{2\pi^2 \ln 2}{m_{\rm e}^5 \cdot ft}\, p_{\rm e}\, E_{\rm e}\, F(Z, E_{\rm e}) \\ &= 0.2167 \times 10^{-43}{\rm cm}^2 \ \frac{p_{\rm e} E_{\rm e}}{{\rm MeV}^2} F(Z, E_{\rm e}) \ ,\end{aligned} \tag{2}$$

where $E_{\rm e} = E_\nu - Q + m_{\rm e}$ is the electron energy,[1] $p_{\rm e}$ is the electron momentum, $F(Z = 7, E_{\rm e})$ is the Fermi factor and the $ft-$value of ^{13}N decay is experimentally determined as $\log(ft/{\rm s})^{\rm exp} = 3.667 \pm 0.001$ [18]. By averaging the cross section over the ^{8}B neutrino spectrum, one obtains $\langle\sigma\rangle = 8.57 \times 10^{-43}{\rm cm}^2$, which is about one order of magnitude larger than the cross section of $\nu_{\rm e}{\rm e} \rightarrow \nu_{\rm e}{\rm e}$ scattering.

The peculiarity of process (1) is that it can be monitored by looking for the delayed coincidence with the positron emitted in the ^{13}N decay:

$${}^{13}{\rm N} \rightarrow {}^{13}{\rm C} + \nu_{\rm e} + {\rm e}^+ \ , \tag{3}$$

[1] We neglected the small recoil energy of the ^{13}N nucleus (of the order of few keV). In this assumption, one has simply $T_{\rm e} = E_{\rm e} - m_{\rm e} = E_\nu - Q$.

which occurs with $\sim 99.8\%$ branching ratio (0.2% of ^{13}N nuclei undergo electron capture) and a decay time $\tau = 862.6$ s. In this case, the visible energy is the sum of the positron kinetic energy and the energy released in e^+e^- annihilation, so that the delayed events have a continuous energy spectrum in the range $[1.02, 2.22]$ MeV. Moreover, in the absence of macroscopic motions in the detector, the ^{13}N nucleus essentially does not move from its original position. The expected displacement due to recoil and diffusion [2] during the decay time τ is, indeed, smaller than the typical detector spatial resolution, $\sigma \sim 10$ cm. This means that the *prompt* event produced by the reaction (1) and the *delayed* event produced by the decay (3) have to be observed essentially in the same position. This condition, as we will see in the following sections, is extremely effective in reducing the background.

Other interaction channels of low energy neutrinos with ^{13}C can, in principle, be considered. First, we discuss the CC transition to ^{13}N excited states. For solar neutrinos, only the lowest excited state (at 3.51 MeV) could be of practical importance. The cross section for this process is about 30% of that for the ground state and it is calculated theoretically with an uncertainty at the level of $30 - 40\%$ [15]. However, the $^{13}N^*(3.51\,\mathrm{MeV})$ decays almost immediately to ^{12}C+p with almost 100% branching ratio [19]. As a consequence, it cannot be discriminated by the coincidence with the delayed events (3). The other relevant process is the neutral current (NC) transition:

$$\nu_x + {}^{13}\mathrm{C} \rightarrow \nu_x + {}^{13}\mathrm{C}^* \ . \tag{4}$$

Here, only the excited state $^{13}C^*(3.68\mathrm{MeV})$ is relevant and the excitation to other levels has negligible cross section. The cross section for this process, averaged over the ^{8}B neutrino spectrum, is $\langle\sigma_{\mathrm{NC}}\rangle = 1.15 \times 10^{-43}\mathrm{cm}^2$ [14,16] and it is affected by about $30 - 40\%$ uncertainty. The process is in principle very interesting since it can give a measure of the total ^{8}B flux and can be also tagged by a monochromatic γ-ray emission back to the ground state. However, the great uncertainty and the low cross section make this process hard to be competitive with the NC measurement made by SNO.

In this Letter, we will mainly focus on the information which can be obtained from reaction (1), which, at present, seems more interesting in view of the larger and much better known cross section, and of the delayed detection tagging with the ^{13}N decay.

[2] Typical value of diffusion coefficients in liquids are $D \sim 10^{-5}$ cm^{2}s^{-1}, which correspond to an average displacement in the time $\tau = 862.6$ s equal to $l_{\mathrm{diff}} = \sqrt{2D\tau} \sim 0.1$ cm.

3 The ^{8}B solar neutrino signal

A neutrino of energy E_ν interacting with ^{13}C through reaction (1) produces an electron with kinetic energy $T_{\rm e} = E_\nu - Q$ (neglecting the ^{13}N recoil). The rate R_ν of prompt events (per unit mass) produced by ^{8}B solar neutrinos in the energy window $[T_{e,1}, T_{e,2}]$ is thus simply given by:

$$R_\nu = n_{^{13}\rm C} \Phi \int_{T_{e,1}+Q}^{T_{e,2}+Q} {\rm d}E_\nu \; \sigma(E_\nu) \lambda(E_\nu) P_{\rm ee}(E_\nu) \; , \tag{5}$$

where $\Phi = 5.79 \times 10^6$ cm^{-2}s^{-1} is the boron neutrino flux [20], $\lambda(E_\nu)$ [3] is the boron neutrino spectrum [21], $\sigma(E_\nu)$ is the interaction cross section and $P_{\rm ee}(E_\nu)$ is the electron neutrino survival probability. In the previous relation, $n_{^{13}\rm C}$ is the number of ^{13}C atoms per unit mass, which depends on the scintillator chemical composition:

$$n_{^{13}\rm C} = \frac{I}{u} \sum_k f_k \frac{X_k}{\mu_k} \; , \tag{6}$$

where $I = 1.07 \times 10^{-2}$ is the isotopic abundance of ^{13}C, $u = 1.661 \times 10^{-33}$ kT is the atomic mass unit, f_k is the mass fraction of the k-th component into the scintillator, X_k the stoichiometric coefficient of carbon in the molecule, and μ_k is the molecular mass of the k-th molecule. KamLAND scintillator is composed by 80% of dodecane ($C_{12}H_{26}$, with a molecular mass $\mu = 170.33$) and 20% of pseudocumene (C_9H_{12}, with a molecular mass $\mu = 120.19$), which correspond to $n_{^{13}\rm C} = 4.60 \times 10^{29}$ kT^{-1}. Borexino is, instead, composed by 100% of pseudocumene, corresponding to $n_{^{13}\rm C} = 4.82 \times 10^{29}$ kT^{-1}. The SNO+ liquid scintillator composition has still to be decided. For simplicity, we will assume, here and in the following, that it will be the same as in Borexino (i. e., 100% pseudocumene).

In Fig. 1 we show the function $\varrho(E_\nu) \propto P_{\rm ee}(E_\nu)\lambda(E_\nu)\sigma(E_\nu)$ (normalized to unity) which gives the relative contribution of neutrinos of different energies to the total signal from reaction (1). The solid line is obtained in the assumption of an undistorted ^{8}B neutrino spectrum (which can be intended as the non oscillatory scenario or a constant suppression of $\nu_{\rm e}$). The dashed line is

[3] A useful approximation for the ^{8}B spectrum is the following:

$$\lambda(E_\nu) = \frac{1}{E_0} \frac{\Gamma(\alpha+\beta)}{\Gamma(\alpha)\Gamma(\beta)} x^{\alpha-1}(1-x)^{\beta-1} \; ,$$

with $x = E/E_0$, $\alpha = 2.92$, $\beta = 3.49$, and $E_0 = 14.8$MeV.

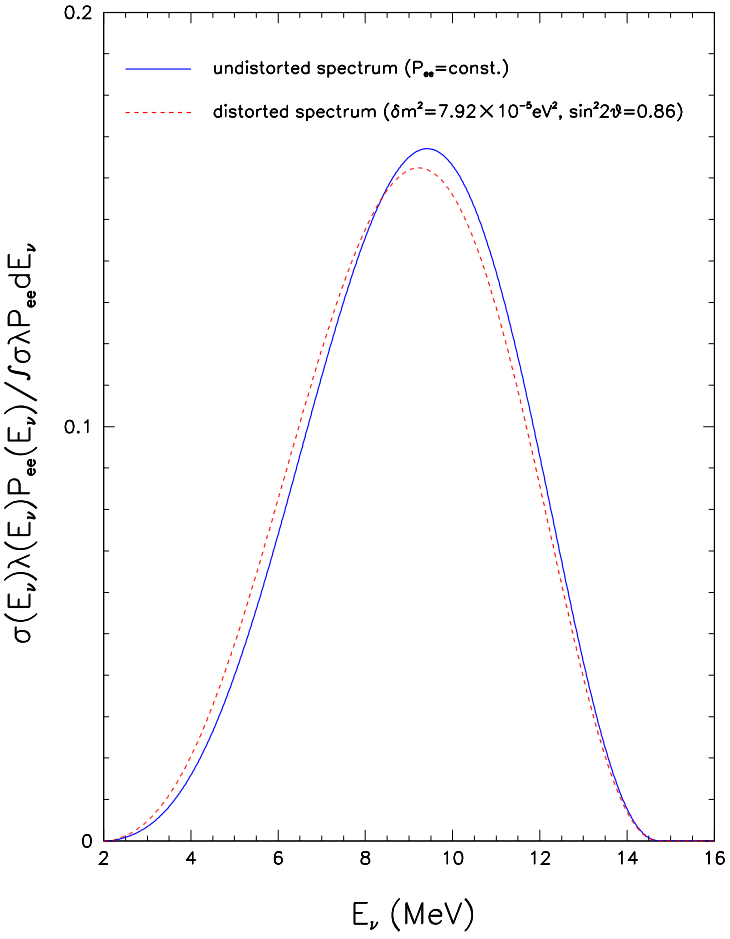

Fig. 1. Relative contribution of neutrinos of different energies to the total signal from reaction (1). Straight line: undistorted ^{8}B neutrino spectrum (constant $P_{\rm ee}$). Dashed line: $\delta m^2 = 7.92 \times 10^{-5}$ eV^2, $\sin^2 2\theta = 0.86$. See the text for more details.

obtained in the assumption of $\nu_{\rm e} \to \nu_{\mu\tau}$ flavor transitions for the following oscillation parameters which are the current best fit (in 2ν) for the whole solar and KamLAND data [11]:

$$\begin{aligned} \delta m^2 &= 7.92 \times 10^{-5}\ {\rm eV}^2\ , \\ \sin^2 2\theta &= 0.86\ . \end{aligned} \tag{7}$$

The electron neutrino survival probability has been calculated taking into account the Mikheyev-Smirnov-Wolfenstein (MSW) effect in the Sun (for sim-

Table 1
Prompt neutrino event rates, delayed energy window efficiency and observed signal event rates for KamLAND and Borexino liquid scintillators. See the text for details.

	Prompt event rate[1]		Delayed energy windows[2]		Signal event rate[1,3]	
	[2.8, 16] MeV	[2.8, 5.5] MeV	[1.02, 2.22] MeV	[1.3, 2.22] MeV	[2.8, 16] MeV	[2.8, 5.5] MeV
KamLAND	23.6	6.3		0.77	12.4	3.3
Borexino	24.7	6.6	1.0		16.8	4.5

[1] counts·kTy^{-1}.

[2] Fraction of ^{13}N decay events in the delayed energy window.

[3] Applied cuts: $\mathcal{R} = 3$, $\mathcal{T} = 2$.

plicity we have not considered the oscillations in the Earth matter). [4] Neglecting the detector energy resolution, the function $f(T_{\rm e}) \equiv \varrho(T_{\rm e} + Q)$ also gives the spectral distribution of solar neutrino events, since detection reaction kinematics implies a one-to-one relation (i. e., $T_{\rm e} = E_\nu - Q$) between the electron and neutrino energies. The event spectrum is, in principle, extremely sensitive to a possible deformation of parent solar neutrino spectrum. In particular, the differences between the two curves in Fig. 1 directly reflect the behavior of the electron neutrino survival probability in LMA scenarios. Namely, the rise of the LMA spectrum (dashed line) with respect to the standard case (solid line) below $E_\nu \sim 7$ MeV ($T_{\rm e} \sim 5$ MeV in terms of electron energy) is due to the transition from vacuum averaged neutrino oscillations at small energies to purely adiabatic transitions at large energies. The observation of this feature would be very important as a final confirmation of matter effect in solar neutrino oscillations. However, it will be extremely hard to observe it in the present detectors, due to the smallness of the expected event rates.

In first two columns of Tab. 1, we show the neutrino event rates (given in counts·kTy^{-1}) expected in KamLAND and Borexino scintillators in the energy windows $[T_{\rm e,1}, T_{\rm e,2}] = [2.8, 16]$ MeV and $[2.8, 5.5]$ MeV, assuming the oscillation parameters in Eq. (7). The lower bound (2.8 MeV) has been chosen to reduce the background from U − Th contamination. The upper bound 5.5 MeV has been chosen to focus on the low energy part of the spectrum, which, as explained above, is particularly interesting and, moreover, is practically unexplored by Super-Kamiokande and SNO. As we can see, the counting rates are of the order of $10 - 20$ counts·kTy^{-1}. Moreover, they will be further reduced by the cuts, essential to reduce the background. However, as we will see in the next sections, the background levels are extremely low so that it will be possible to extract the solar neutrino signal with a reasonable uncertainty. We remark that the proposed measure does not require any modification of the present experimental set-up and, although with a larger uncertainty, can be complementary to those coming from SNO and Super-Kamiokande.

[4] A simple and accurate approximation to calculate the adiabatic MSW survival probability can be found in [22].

4 Tagging the events

In order to reduce the background, we can take advantage of the time and space coincidence of neutrino events with the positron emitted in the ^{13}N decay. A candidate prompt event will be tagged as signal only if followed by a *delayed* event in the energy window $[1.02, 2.22]$ MeV, within a time interval $\Delta t = \mathcal{T}\tau$ (where $\tau = 862.6$ s is the ^{13}N decay time), and inside a sphere of radius $r = \mathcal{R}\sigma$ from the prompt event detection point (where $\sigma \sim 10$ cm is the typical detector spatial resolution, see, e. g., [10]). The signal event rate is thus given by:

$$S = R_\nu \cdot \epsilon(\mathcal{T}, \mathcal{R}) \ , \tag{8}$$

where the global efficiency of the coincidence, $\epsilon(\mathcal{T}, \mathcal{R})$, is determined by the combined efficiency for the cut in space, $\xi(\mathcal{R})$, and in time, $\eta(\mathcal{T})$:

$$\epsilon(\mathcal{T}, \mathcal{R}) = \xi(\mathcal{R}) \cdot \eta(\mathcal{T}) \ . \tag{9}$$

The function $\eta(\mathcal{T})$ is simply equal to the probability that the ^{13}N nucleus decays within the time $\Delta t = \mathcal{T}\tau$:

$$\eta(\mathcal{T}) = 1 - \exp(-\mathcal{T}) \ . \tag{10}$$

The function $\xi(\mathcal{R})$ is instead the probability that the prompt event and the delayed event, which are assumed to occur in the same position, are detected at a distance smaller than $r = \mathcal{R}\sigma$. Modelling the detector spatial resolution with a gaussian function, one obtains: [5]

$$\xi(\mathcal{R}) = \frac{\int_0^{\mathcal{R}} \mathrm{d}x \ x^2 \exp(-x^2/4)}{\int_0^{\infty} \mathrm{d}x \ x^2 \exp(-x^2/4)} = \mathrm{erf}\left(\frac{\mathcal{R}}{2}\right) - \sqrt{\frac{1}{\pi}}\mathcal{R} \exp\left(-\frac{\mathcal{R}^2}{4}\right) \ . \tag{11}$$

We remark, that the above equation is valid in the assumption that the displacement between the point where ^{13}N is created and the point where it decays is small with respect to σ. For that to happen, the macroscopic motions

[5] If we model the detector spatial resolution with a gaussian function $f(\mathbf{x}, \mathbf{x}_0) \propto \exp[-(\mathbf{x} - \mathbf{x}_0)^2/2\sigma^2]$, where $\mathbf{x}_0$ is the true position of the event and $\mathbf{x}$ is the *observed* position of the event, the probability that the prompt event is observed in the position $\mathbf{x}_\mathrm{p}$ and the delayed in the position $\mathbf{x}_\mathrm{d}$ can be cast as $\mathrm{d}P(\mathbf{x}_\mathrm{p}, \mathbf{x}_\mathrm{d}) = f(\mathbf{x}_\mathrm{p}, \mathbf{x}_0) f(\mathbf{x}_\mathrm{d}, \mathbf{x}_0) \, \mathrm{d}^3\mathbf{x}_\mathrm{p} \mathrm{d}^3\mathbf{x}_\mathrm{d} \propto \exp\left[-(\mathbf{r} + \mathbf{y})^2/4\sigma^2\right] \mathrm{d}^3\mathbf{r} \, \mathrm{d}^3\mathbf{y}$, where $\mathbf{r} = \mathbf{x}_\mathrm{p} - \mathbf{x}_\mathrm{d}$ and $\mathbf{y} = \mathbf{x}_\mathrm{p} + \mathbf{x}_\mathrm{d} - 2\mathbf{x}_0$. Actually, only the distance $r = |\mathbf{r}|$ is observable, so that, integrating $\mathbf{r}$ on a sphere of radius $\mathcal{R}\sigma$ and $\mathbf{y}$ on $\mathbf{R}^3$, one obtains Eq. (11).

in the liquid scintillator have to be sufficiently slow. This can be achieved, for example, by maintaining a small temperature gradient pointing upward everywhere in the detector. KamLAND data show that the measured average displacement of the diffusive ^{222}Rn over its 5.5 d mean life is less than 1 m [23]. Therefore, the assumption that ^{13}N nuclides displacement over their 15 minutes lifetime can be kept smaller than detector resolution seems justified.

Finally, we consider the possibility that the delayed energy window is reduced with respect to the full energy range ($[1.02, 2.22]$ MeV) of ^{13}N decay spectrum. In this case the signal event rate is given by:

$$S = R_\nu \cdot \epsilon(\mathcal{T}, \mathcal{R}) \cdot \mathcal{B}(E_1, E_2) = R_\nu \cdot \epsilon(\mathcal{T}, \mathcal{R}) \cdot \int_{E_1}^{E_2} \mathrm{d}E_\mathrm{d}\, \chi(E_\mathrm{d}) \ , \tag{12}$$

where $\mathcal{B}(E_1, E_2)$ is the fraction of decay events in the adopted energy window $[E_1, E_2]$ [$\chi(E)$ is the normalized ^{13}N decay spectrum].

In last two columns of Tab. 1, we show the signal event rates (given in counts·kTy^{-1}) expected in the KamLAND and Borexino liquid scintillators, after that the efficiency cuts are applied. Here, for illustrative purposes, we consider a time cut at $\mathcal{T} = 2$ and a space cut at $\mathcal{R} = 3$, which correspond to a global efficiency $\epsilon(\mathcal{R}, \mathcal{T}) = 0.68$. It is clear, however, that the cuts must be optimized according to each detector's capabilities and performances. For the KamLAND detector, moreover, we restrict the delayed energy window to $[E_1, E_2] = [1.3, 2.22]$ MeV in order to reduce the background from ^{210}Bi originated by the decay of ^{210}Pb that can be either produced by build-up due to ^{222}Rn contamination in the liquid scintillator or caused by an intrinsic impurity. [6] This reduces further the efficiency by a factor 0.77. For Borexino (and SNO+), we consider instead the full range $[1.02, 2.22]$ MeV, assuming that the ^{210}Bi background contribution will be further reduced, since this is a pre-requisite for the observation of sub-MeV solar neutrinos. [7]

As a final result, the expected signal event rates are at the level of $10 - 20$ counts·kTy^{-1}. In order to observe such low counting rates, one clearly needs detectors with sufficiently low background levels (and, of course, efficient background rejection). Present detectors, as we shall see in the next section, already satisfy this requirement.

[6] At present ^{210}Pb is an important contamination in KamLAND which will be removed by purification to allow solar neutrinos detection.

[7] If the detector has an intrinsic efficiency ϵ_p (ϵ_d) for the prompt (delayed) window, the global efficiency is further reduced by a factor $\epsilon_\mathrm{p} \cdot \epsilon_\mathrm{d}$. We assume for simplicity $\epsilon_\mathrm{p} = \epsilon_\mathrm{d} = 1$.

Table 2
Rate of background events in the prompt and delayed windows and rate of fake coincidences.

	Prompt energy window(s)[1]		Delayed energy window[1]	Fake coincidences[1,2]	
KamLAND	[2.8, 16] MeV	[2.8, 5.5] MeV	[1.3, 2.22] MeV	[2.8, 16] MeV	[2.8, 5.5] MeV
U − Th	1168	1168	1533		
Cosmogenics (no ^{12}B)	20779	15654	261555		
Elastic scattering	967	558	398		
Total	22914	17381	263486	29.1	22.1
Borexino	[2.8, 16] MeV	[2.8, 5.5] MeV	[1.02, 2.22] MeV	[2.8, 16] MeV	[2.8, 5.5] MeV
U − Th	1168	1168	2373		
Cosmogenics (no ^{12}B)	2968	2236	54800		
Elastic scattering	1004	577	3460		
Total	5140	3981	60632	1.69	1.31
SNO+	[2.8, 16] MeV	[2.8, 5.5] MeV	[1.02, 2.22] MeV	[2.8, 16] MeV	[2.8, 5.5] MeV
U − Th	1168	1168	2373		
Cosmogenics (no ^{12}B)	32	24	583		
Elastic scattering	1004	577	3640		
Total	2203	1768	6416	0.08	0.06

[1] counts·kTy^{-1}.

[2] Applied cuts: $\mathcal{R} = 3$, $\mathcal{T} = 2$.

5 The background

There are three main sources of background for the proposed measure. These are:

i) Internal background due to U − Th contamination and to contamination from long lived radon daughters out of secular equilibrium with ^{238}U (in particular ^{210}Pb);
ii) Cosmogenic background due to muon-induced production of radioactive nuclides, such as ^{11}C, ^{10}C , etc.;
iii) Elastic $\nu-$e scattering by solar neutrinos.

These background sources are well known, so that it is possible to perform a detailed analysis of their relevance. This is clearly important, because it allows to make a realistic estimate. We remark, however, that the real background level will be *measured* directly by the experiments with great accuracy, being the background event rate much larger than the signal event rate both in the prompt and delayed energy window (before space and time cuts are applied).

In Tab. 2, we show the contribution of each background source to the total background rates (per unit mass) in KamLAND, Borexino and SNO+. We have assumed that the U − Th contamination in the detectors is at the 10^{-17} g/g level, which correspond to the *present* contamination in the KamLAND detector [17]. The internal background due to the elastic scattering of solar neutrinos on electrons has been evaluated assuming $\nu_{\rm e} \to \nu_{\mu\tau}$ flavor oscillations with the oscillation parameters given in Eq. (7). Finally, the cos-

Table 3
Depth, residual muon flux and average muon energy in the three undergound locations considered in the Letter (see [25] for details).

	Depth (m.w.e.)	ϕ_μ ($m^{-2}d^{-1}$)	$\langle E_\mu \rangle$ (GeV)
Kamioka	2700	230.4	285
Gran Sasso	3800	28.8	320
SNOlab	6000	0.288	350

mogenic contribution has been obtained by rescaling the results of [24], which are relative to Borexino, also to KamLAND and SNO+. This can be done by considering that the muon induced background R_μ in a given experiment scales as $R_\mu \propto n_{^{12}C} \Phi_\mu \langle E_\mu \rangle^\alpha$, where Φ_μ is the muon flux at the experimental site, $\langle E_\mu \rangle$ is the average muon energy, $n_{^{12}C}$ is the number of ^{12}C nuclei per unit mass in the scintillator (the ^{12}C is the most relevant target for muon induced radioactive nuclei production in liquid organic scintillators) and $\alpha = 0.73$. [8] From the data in Tab. 3 (see [25] for details) we calculate that the cosmogenic background is ~ 7 times *larger* in KamLAND than in Borexino, while is ~ 94 times *lower* in SNO+.

From Tab. 2 we see that cosmogenic background is the dominant component for KamLAND and Borexino both in the prompt and delayed window, while it give only a minor contribution to the total background in SNO+. It is interesting to give a closer look at the various cosmogenic background sources. The relevant cosmogenic nuclei and their half-lives are reported in Tab. 4. We see that only ^{11}C and ^{10}C nuclei have a long lifetime. The background coming from the other cosmogenics can be efficiently rejected simply extending the muonic veto to few seconds after the muon passage through the detector. However, in order to avoid further losses of efficiency due to the veto dead-time, we rejected only the background events coming from the (fast) decay of ^{12}B. In the last four rows of Tab. 4 we show the event rates (given in counts·kTy^{-1}) expected in Borexino [24] for the four energy windows considered in this work. We see that the main contribution to cosmogenic background in the prompt energy windows come from ^{10}C, while the dominant source in delayed windows is provided by ^{11}C nuclides. It was recently shown [25] that ^{11}C-induced background can be greatly reduced by a three fold coincidence with the parent muon track and the subsequent neutron capture on protons. However, in order to be extremely conservative, we have not considered this possibility. [9]

[8] The cosmogenic production cross section scales with the energy as $\sigma \propto E_\mu^\alpha$ with $\alpha \sim 0.73$ [24].

[9] An additional background not included above is provided by the interaction of cosmogenic protons with ^{13}C, according to ^{13}C(p,n)^{13}N. These events are potentially dangerous because, being followed by the decay of the produced ^{13}N, they cannot be discriminated by the coincidence (a rejection is, anyhow, possible by looking at the subsequent neutron capture on protons). We have estimated, by MonteCarlo

Table 4
Main cosmogenic nuclei, their half-lives, and event rates (in counts·kTy^{-1}) in the Borexino detector [24] for the relevant energy windows considered in this Letter.

	β^+ emitters				β^- emitters		
	^{11}C	^{10}C	^{9}C	^{8}B	^{12}B	^{8}Li	^{6}He
$T_{1/2}$ (s)	1218	19.3	0.127	0.770	0.0202	0.840	0.807
[2.8, 16] MeV	0	2021	275	389	2933	241	42
[2.8, 5.5] MeV	0	2021	40	82	911	51	42
[1.02, 2.22] MeV	52630	1637	2	5	138	7	519
[1.3, 2.22] MeV	35316	1637	2	5	119	6	399

In the last two columns of Tab. 2, we show the background in the prompt energy windows after the coincidence criteria are applied. This is obtained by considering that the probability to have a background event in the delayed energy window when space and time cuts are applied is simply equal to the average number of delayed background events during the time interval $\Delta t = \mathcal{T}\tau$ and inside the spherical volume $V = (4/3)\pi(\mathcal{R}\sigma)^3$, being this number much smaller than one. [10] The rate of fake coincidences B is thus given by:

$$B = (B_{\rm p} B_{\rm d} \rho) \left[\frac{4}{3}\pi(\mathcal{R}\sigma)^3 \mathcal{T}\tau\right] \ , \tag{13}$$

where $B_{\rm p}$ and $B_{\rm d}$ are the prompt and delayed background rates (per unit mass), ρ is the liquid scintillator density (equal to $\rho = 0.78\,{\rm g/cm^3}$ for the KamLAND scintillator and $\rho = 0.88\,{\rm g/cm^3}$ for the Borexino scintillator) and we have taken $\mathcal{R} = 3$ and $\mathcal{T} = 2$. We see that, despite of the large number of background events (several thousands per kTy) in the prompt and delayed energy window, the fake coincidences are rare (tenth per kTy in KamLAND, few per kTy in Borexino or almost absent in SNO+), and comparable or lower than the expected signal. For this reason we think that a measure of the ^{8}B solar neutrino flux is feasible.

simulations, that this background component is negligible, being the cosmogenic proton interaction rate with ^{13}C of the order $\sim 10^{-2}$ kTy^{-1} in Borexino.

[10] The probability to have at least one background event inside a certain (spatial and/or temporal and/or energy) window should be calculated by means of a Poissonian distribution. However, since the number of background events is very small, the probability is practically equal to the average number of events in the considered window.

6 Expected sensitivity and future prospects

Since real and fake coincidences are indistinguishable, the number of signal events N_S has to be obtained from the difference between the total number of observed events N_T and the number of background events N_B:

$$N_S \equiv S \cdot \mathcal{E} = N_T - N_B = N_T - B \cdot \mathcal{E} \ , \tag{14}$$

where S is the signal event rate, B is the background event rate and $\mathcal{E}$ is the total detector exposure. The uncertainty of the number of signal events ΔN_S is obtained propagating the error in Eq. (14):

$$\Delta N_S = \sqrt{N_T + (\Delta B \cdot \mathcal{E})^2} \ , \tag{15}$$

where we assumed that the total number of events is affected by a Poissonian uncertainty $\Delta N_T = \sqrt{N_T}$ and we combined in quadrature the errors. Dividing by N_S we obtain the fractional uncertainty δS of the signal rate:

$$\delta S \equiv \frac{\Delta S}{S} = \sqrt{\frac{1+r}{S \cdot \mathcal{E}} + r^2 \, \delta B^2} \ , \tag{16}$$

where $r = B/S$ is *background-to-signal* ratio and δB is the fractional uncertainty of the background rate.

As anticipated in the previous section, the background will be directly measured by the experiments. More precisely, one measures the prompt and the delayed background rates and, then, determines the final background rate B through Eq. (13). The uncertainty δB can, thus, be estimated as:

$$\delta B = \sqrt{\delta B_{\rm p}^2 + \delta B_{\rm d}^2} = \frac{1}{\mathcal{E}^{1/2}} \sqrt{\frac{1}{B_{\rm p}} + \frac{1}{B_{\rm d}}} \tag{17}$$

where we considered that the fractional uncertainties of the prompt and delayed background rates are given by $\delta B_{\rm p,d} = [B_{\rm p,d} \cdot \mathcal{E}]^{-1/2}$,as prescribed by Poissonian statistics.By using Eq. (17), Eq. (16) can be cast as:

$$\delta S = \frac{1}{\sqrt{S \cdot \mathcal{E}}} \sqrt{(1+r) + \left[\frac{S}{B_{\rm p}} + \frac{S}{B_{\rm d}} \right] r^2} \ . \tag{18}$$

It is immediately evident that the second term in the square root of the above expression is always negligible, being the ratios $r^2 S/B_{\rm p,d}$ of the order of 10^{-3}

Table 5
Background-to-signal ratio and expected sensitivity for KamLAND, Borexino and SNO+ for 1kTy of exposure. See the text for details.

	Background-to-signal ratio[1]		Expected sensitivity[1]		Expected sensitivity (optimized)[2]	
	[2.8, 16] MeV	[2.8, 5.5] MeV	[2.8, 16] MeV	[2.8, 5.5] MeV	[2.8, 16] MeV	[2.8, 5.5] MeV
KamLAND[3]	2.35	6.73	51.9%	152.2%	51.2%	145.4%
Borexino[4]	0.100	0.291	25.6%	53.6%	23.7%	52.2%
SNO+[4]	0.005	0.014	24.4%	47.5%	20.6%	40.9%

[1] $\mathcal{R} = 3$ and $\mathcal{T} = 2$.

[2] Space and time cuts are optimized to minimize δS in each detector, see the text.

[3] Delayed energy window: [1.3, 2.22] MeV.

[4] Delayed energy window: [1.02, 2.22] MeV.

or less in the various detectors. This means that the contribution of the background uncertainty to the total error budget is always negligible:

$$\delta S \simeq \sqrt{\frac{1+r}{S \cdot \mathcal{E}}} \, . \tag{19}$$

This situation is, in principle, favorable. The fractional uncertainty δS scales as $\mathcal{E}^{-1/2}$, and, thus, it is possible to obtain a good sensitivity if the detector exposure is large enough. In the following we assume $\mathcal{E} = 1$ kTy.

In the first two columns of Tab. 5 we show the background-to-signal ratio r for the three experiments under study in the two energy windows $[2.8, 16]$ MeV and $[2.8, 5.5]$ MeV, assuming a space cut $\mathcal{R} = 3$ and a time cut $\mathcal{T} = 2$. In the third and fourth columns, we show the corresponding sensitivity δS, calculated according to Eq. (19), assuming a total exposure $\mathcal{E} = 1$ kTy. In the last two columns, we give the minimal values for δS obtained by choosing the optimal values of $\mathcal{R}$ and $\mathcal{T}$ which minimize the quantity $(1 + r)/S$ in each experiment. [11] Clearly, the lower is the background level in the detector, the larger is the space-time window which has to be considered. In KamLAND the optimal sensitivity is obtained with $\mathcal{R} = 2.82$ and $\mathcal{T} = 1.65$ in the energy window $[2.8, 16]$ MeV and $\mathcal{R} = 2.64$ and $\mathcal{T} = 1.44$ in the energy window $[2.8, 5.5]$ MeV. Larger cuts are preferable for Borexino and SNO+ (of the order of $\mathcal{R} \sim 5$ and $\mathcal{T} \sim 5$). However, the choice of cuts is not crucial these (less noisy) detectors and the sensitivity does not change dramatically if we take tighter cuts.

In KamLAND, due to the large cosmogenic contribution, the background-to-signal ratio is equal to about 2.5 in the energy window $[2.8, 16]$ MeV (while it is equal to about 7 if we restrict to $[2.8, 5.5]$ MeV). This corresponds to an expected sensitivity δS equal to about 50% in one year of data taking (assuming $\sim$1 kT fiducial mass). We remind that KamLAND has already

[11] This exercise have to be done numerically, since $\mathcal{R}$ and $\mathcal{T}$ enter in Eq. (19) in a non-trivial way.

analyzed data for a total exposure $\mathcal{E} = 0.766$ kTy [8], corresponding to ~ 18 solar neutrino events in the window $[2.8, 16]$ MeV which can be extracted with about 60% uncertainty. [12] Despite the large uncertainty, we believe that this measure would, anyhow, represent a milestone, since it would be the first observation of solar neutrinos into liquid scintillator detectors. We hope that the KamLAND collaboration will try to extract this piece of information from their own set of data.

In Borexino and in SNO+, due to the larger depth of the experimental sites, the background-to-signal ratio is much less than one. The sensitivity is thus only limited by the statistical error of the signal events. The low background level allows to explore with sufficient accuracy the energy windows $[2.8, 5.5]$ MeV for which, at present, we have no direct information. This also indicates that, in these experiments, it will be possible to decrease the lower bound of the energy windows (2.8 MeV) with only a moderate decrease of the expected sensitivity.

We remark that, even if the background is negligible, the low expected counting rates do not allow to observe a possible distortion of solar neutrino event spectrum, unless the ^{13}C abundance is enriched and/or one considers gigantic detectors. In principle, ^{13}C enrichment is possible. [13] However, the current separation techniques probably do not allow a massive production of this isotope. For this reason, we do not consider in detail this possibility. One should note, however, that even a partial enrichment (e. g., corresponding to a ^{13}C abundance of the order $20 - 30\%$) could allow to obtain important results, like e. g., the high accuracy determination of the solar neutrino spectrum down to energies equal to about $E_\nu \sim 3$ MeV (or the observation of *hep* solar neutrinos).

Finally, we briefly discuss the perspectives for gigantic liquid scintillator detectors planned in the future. In particular a ≥ 30 kT detector, the Low Energy Neutrino Astrophysics (LENA), has been proposed [13]. The site proposed for the experiment is Pyhäsalmi mine in Finland at a depth comparable to that of Borexino ($\sim$ 4000 m.w.e.). This means that the cosmogenic background will be sufficiently low for the proposed measure. The scintillator should be composed mainly by PXE ($C_{16}H_{18}$, with a molecular mass $\mu = 210.31$ and a density density $\rho = 0.998$ g/cm^3), but, of course, the final composition has yet to be decided. It is clear that, in such a large detector, it will be very hard to keep the internal background low. However, the gain in statistics will probably overcompensate this limitation. To give an example, in one year of data taking with a fiducial mass equal to 30 kT, one obtains a better sensitivity than in

[12] Of course, with the proposed cuts, only about 9 of these events would be tagged as candidate.
[13] The ^{13}C is mainly used in health diagnostic, since it has a specific NMR signature.

SNO+ (with 1 kT fiducial mass), even assuming a background-to-signal ratio of the order of ten. For this reason, we believe that the LENA detector has the capability to perform a precise measure of the ^{8}B flux (comparable to that provided by Super-Kamiokande and/or SNO) in a few years of data taking.

7 Summary and conclusions

In this Letter we have discussed the possibility to detect ^{8}B solar neutrinos by using the ν_e CC-interaction with ^{13}C nuclei naturally contained in organic liquid scintillators. The proposed detection process has a low threshold ($Q = 2.22$MeV) and large and well-know cross section. Moreover, one can take advantage of the subsequent decay of the produced ^{13}N nuclei to discriminate neutrino events from the background.

We have calculated the expected event rates (of the order of ~ 20 kTy^{-1}) for KamLAND, Borexino and an hypothetical Borexino-like experiment situated at SNOlab (SNO+). Moreover, we have evaluated thoroughly all the possible sources of (external and internal) background in the three considered detectors. We have shown that the background-to-signal ratio is ~ 2 in KamLAND, while is much less than 1 in Borexino and SNO+.

Finally, we have calculated the expected sensitivity for the various experiments. Assuming an exposure equal to $\mathcal{E} = 1$ kTy, the solar neutrino signal can be extracted with uncertainty of the order of $\sim 50\%$ in KamLAND and $\sim 20 - 25\%$ in Borexino and SNO+. The expected sensitivity scales as $\mathcal{E}^{-1/2}$, since background is directly measured by the experiments. Gigantic (such as LENA) and/or enriched detectors, having a much larger statistics, will have the possibility to perform a very precise measurement of the ^{8}B neutrino flux.

It should be stressed that the proposed measure does not require any modification of the standard experimental set-up. The KamLAND detector should be able to extract about ~ 18 ^{8}B solar neutrino events from the already collected data (corresponding to a total exposure equal to 0.766 kTy).

Acknowledgments

The authors are grateful to many participants of the NOW 2004 workshop for interesting discussions, where this work has begun. We thank C. Galbiati and D. Franco for helpful discussions on ^{13}C(p,n)^{13}N background, and L. Oberauer and M. Chen for reading the manuscript and useful comments. F. V. also

thanks G. Fiorentini for useful discussions and comments. This work is supported by the Italian Ministero dell'Istruzione, Università e Ricerca (MIUR) and Istituto Nazionale di Fisica Nucleare (INFN) through the "Astroparticle Physics" research project.

References

[1] Homestake Collaborations, B. T. Cleveland *et al.*, Astrophy. J. **496**, 505 (1998).

[2] Gallex Collaboration, W. Hampel *et al.*, Phys. Lett. **B447**, 127 (1999).

[3] GNO Collaboration, M. Altmann *et al.*, Phys. Lett. **B490**, 16 (2000).

[4] SAGE Collaboration, J. N. Abdurashitov *et al.*, J. Exp. Theor. Phys. **95** 181 (2002).

[5] Kamiokande Collaboration, K. S. Hirata *et al.*, Phys. Rev. Lett. **65**, 1297 (1990).

[6] Super-Kamiokande Collaboration, S. Fukuda *et al.*, Phys. Rev. Lett. **86**, 5651 (2001).

[7] SNO Collaboration, Q. R. Ahmad *et al.*, Phys. Rev. Lett. **89**, 011301 (2002).

[8] KamLAND Collaboration, T. Araki *et al.*, Phys. Rev. Lett. **94**, 081801 (2005).

[9] Borexino Collaboration, G. Alimonti *et al.*, Astrop. Phys. **8**, 141 (1998); *ibid.*, Nucl. Instrum. Meth. **A406**, 411 (1998).

[10] Borexino Collaboration, G. Alimonti *et al.*, Astrop. Phys. **16**, 205 (2002).

[11] G. L. Fogli, E. Lisi, A. Palazzo, and A. M. Rotunno, Phys. Lett. **B623**, 80 (2005).

[12] See, e. g., M. Chen, proceedings of "NOW 2004", Neutrino Oscillation Workshop (Otranto, Italy, 2004), Nucl. Phys. B, Proc. Suppl. **145**, 65 (2005).

[13] See, e. g., L. Oberauer, F. von Feilitzsch, and W. Potzel, proceedings of 8th International Workshop on Topics in Astroparticle and Underground Physics (TAUP 2003), (Seattle, Washington, U.S.A., 2003), Nucl. Phys. B, Proc. Suppl. **138**, 108 (2005); L. Oberauer Mod. Phys. Lett. **A19**, 337 (2004); for a recent review see also the talk by F. von Feilitzsch at "CuTAPP" workshop, Current Topics in Astroparticle Physics, (Ringberg, Germany, 2005). Slides available at the conference home page, www.mppmu.mpg.de/common/seminar/conf/conf2005/cutapp/ .

[14] J. Arafune, M. Fukugita, Y. Kohyama, and K. Kubodera, Phys. Lett. B **217**, 186 (1989).

[15] M. Fukugita, Y. Kohyama, K. Kubodera, and T. Kuramoto, Phys. Rev. C **41**, 1359 (1990).

[16] K. Kubodera and S. Nozawa, Int. J. Mod. Phys. E **3**, 101 (1994).

[17] KamLAND Collaboration, K. Eguchi *et al.*, Phys. Rev. Lett. **90**, 021802 (2003).

[18] F. Ajzenberg-Selove, Nucl. Phys. **A360**, 1 (1981); **A449**, 1 (1986); **A523**, 1 (1991).

[19] H. Fujimura *et al.*, Phys. Rev. C **69** 064327 (2004).

[20] J. N. Bahcall and M. H. Pinsonneault, Phys. Rev. Lett. **92**, 121301 (2004).

[21] Tables of the ^{8}B spectrum can be found at the J. N. Bahcall home page, www.sns.ias.edu/ jnb/, see "Neutrino Software and Data".

[22] P. C. de Holanda, W. Liao, A. Yu. Smirnov, Nucl. Phys. **B** 702, 307 (2004).

[23] J. Shirai (for the KamLAND Collaboration), in the proceedings of "Neutrino 2002", 20th International Conference on Neutrino Physics and Astrophysics (Munich, Germany, 2002), Nucl. Phys. B, Proc. Suppl. **118**, 15 (2003).

[24] T. Hagner, R. von Hentig, B. Heisinger, L. Oberauer, S. Schonert, F. von Feilitzsch, and E. Nolte, Astropart. Phys. **14**, 33 (2000).

[25] C. Galbiati, A. Pocar, D. Franco, A. Ianni, L. Cadonati, and S. Schonert, Phys. Rev. C 71, 055805 (2005); see also D. Franco, for the Borexino collaboration, proceedings of "NOW 2004", Neutrino Oscillation Workshop (Otranto, Italy, 2004), Nucl. Phys. B, Proc. Suppl. **145**, 29 (2005).